City, University of London Institutional Repository

Multi-mode traffic-induced vibrations in composite ladder-deck bridges under heavy moving vehicles

A. Camara, A.M. Ruiz-Teran

Department of Civil and Environmental Engineering. Imperial College London. South Kensington Campus. Exhibition Rd, London SW7 2AZ, United Kingdom

Abstract

Composite (steel-concrete) ladder-decks represent one of the most common solutions in road bridges nowadays. In these structures the Serviceability Limit State (SLS) of vibrations is traditionally ignored or roughly addressed by means of simple static deflection-based approaches, inherently assuming that the vibrations are controlled by the fundamental longitudinal mode. This work demonstrates that a wide range of high-order vibrational modes, involving the transverse flexure of the slab between longitudinal girders, govern the accelerations recorded in the deck and inside the vehicles. In addition, a new methodology for analysing the vehicle-bridge interaction is proposed, including the approaching platforms, the transition slabs, and the bridge joints. The results suggest that the riding comfort for vehicle users is specially affected by direct effects on the wheels, like the road roughness and possible construction misalignments at the bridge joints, as well as low-frequency vibrations coming from the deck in short or slender bridges. The filtering effects resulting from the average of the response in time and in space when calculating the root mean square acceleration are also explored, and new design parameters are provided. In addition, several structural features (such as the depth and spacing of the longitudinal and transverse steel

Email addresses: `acamara@ciccp.es` (A. Camara), `a.ruiz-teran@imperial.ac.uk` (A.M. Ruiz-Teran)

beams, the thickness of the concrete slab, and the stiffness of the cantilever cross beams at the diaphragm sections) have been studied, and a set of new design criteria have been established. It has been demonstrated that the transverse flexibility of the deck (specially influenced by the support conditions and the slab thickness) is critically important for the users' (pedestrians and vehicle passengers) comfort, as it controls the aforementioned high-order vibrational modes which govern the dynamic response.

1. Introduction

Modern road bridge designs tend to be lighter and slenderer. As a result, vibrations have become more of a concern in bridge design. A realistic approach to assess the vibration induced by traffic loading is not currently available. Traditionally, the limitation of the superstructure vibrations in the design of road bridges has been indirectly performed by limiting the deflection under statically applied live-loads [1]. This approach dates back to the early 1930s when more rigorous dynamic analyses were not available, and it is based on the general agreement that the accelerations are proportional to the deflections. Today, static methods to assess the structural vibrations represent the most common design approach due to their simplicity and tradition, but they are widely criticised [1, 2, 3]. Already in 1958, a survey committed by the American Society of Civil Engineering (ASCE) evidenced no clear structural basis for the deflection limits and highlighted the need to reexamine them [4]. More importantly, vibration criteria for serviceability limit states should be derived by considering human perception rather than simply structural performance [5]. The vertical acceleration sensed by users, and not the live load deflection of the deck, governs their perception to vibrations, being the most important parameter affecting discomfort [1, 2, 6]. As an attempt to estimate the vertical acceleration in the deck from its dynamic deflection, different pseudo-static methods have been proposed [3, 7]. However, the deflection-based methods inherently assume that the structure is controlled by the fundamental mode of vibration. This was proved wrong in slender under-deck cable-stayed bridges [8], as well as in high-performance

2

steel multi-girder bridges [9], and it is evidenced again for conventional composite ladder-deck girders in the present work.

In conventional short and medium span road bridges the most important source of vibration is the traffic live load, in particular heavy vehicles. Most of the research works to date ignore the vibrations perceived by the people inside the vehicle as they seldom notice the bridge vibration [7]. However, in highway bridges pedestrians are not normally expected to walk along the bridge and therefore the only users are those inside the vehicles. People in the vehicles could feel discomfort if they are stationary, as observed by Oehler [10], or circulating at reasonable velocities through pavements with poor maintenance [8]. The simplest dynamic analysis to obtain the time-history acceleration record is to model the vehicle action as point moving loads. Nevertheless, this simplified approach has important shortcomings: (1) the effect of the pavement roughness cannot be included and it is very important for the vibration assessment [8, 11, 12, 13], (2) the vibration in the vehicle and its interaction with the deck is ignored, and (3) the hammering effect caused by the initial bounce of the vehicle on its suspension when crossing the deck joint at the abutments, which represent a major source of vibrations, is not captured. The most rigorous way to account for these three effects is to represent the Vehicle-Bridge Interaction (VBI) by means of a Multi-Degree-Of-Freedom (MDOF) system of the vehicle and its contact with the deck surface through the wheels [8, 11, 14].

Pavement irregularities in VBI models are included as vertical displacement records imposed on the vehicle wheels that represent the roughness profiles. These profiles are usually generated by means of a zero-mean stationary Gaussian random process through an inverse Fourier transformation based on a Power Spectral Density (PSD) function [12, 13, 15]. The Motor Industry Research Association report in 1969 [16] introduced one of the first attempts to describe the road roughness through an idealisation of the PSD function. Today, the recommendations of ISO 8608 [17] are broadly employed to define the PSD function. It is essential to select realistic values for the lower and upper cut-off frequencies (n_1 and n_N respectively), as well as for the frequency resolution (Δn). The majority of the research works employ an upper cut-off frequency of $n_N = 10$ cycle/m [11, 18, 19], as an attempt to indirectly take into account the filtering effect of the vehicle wheels. There are more rigorous ways to explicitly consider this effect, for example defining the wheel contact surface [20] or a rigid disk model that accounts for the real wheel dimensions [8, 21]. Previous research works usually consider the lower

3

cut-off frequency as $n_1 = 0.01$ cycle/m. However, for bridge applications Henchi *et al.* [22] recommend roughness profiles related to the span of the bridge (L) so that $n_1 = 1/(2L)$, which is supported by the surfacing procedure. The frequency resolution is not usually reported but several authors [14, 22] adopt: $\Delta n = 1/L_{prof}$, where L_{prof} is the total length of the profile.

Several direct and indirect factors influence the pedestrian perception of vibration when crossing a bridge [23, 24, 25, 26]. Some of these factors are subjective and consequently admissible vibration limits vary widely among individuals, which makes the establishment of realistic comfort criteria as challenging as urgently needed. Among these factors, the exposure time is significantly important. It is evident that the level of vibration that users can accept as admissible is much higher if the exposure time is shorter, as it was measured by Griffin and Whitham [27]. The first acceleration-based comfort criteria were based on peak acceleration limits [3, 28], which is questionable. Due to the hammering effect of the vehicle when it enters and leaves the bridge, high vertical acceleration peaks have been measured by [29] at the deck nearby the girder ends, far exceeding any admissible limit. In addition, the peak accelerations associated with uncomfortable levels in some laboratory tests result in unrealistically severe evaluations in buildings, which is not correlated with observation [30]. The results obtained in the present paper point at the same direction. The majority of the comfort criteria used historically are based on maximum Root Mean Square accelerations, much simpler to evaluate experimentally than the peak value:

$$a_{\mathrm{RMS}}(t) = \sqrt{\frac{1}{T_2 - T_1} \int_{T_1}^{T_2} [a(t)]^2 \mathrm{d}t} \tag{1a}$$

$$\mathrm{RMS} = \max[a_{\mathrm{RMS}}(t)] \tag{1b}$$

where $a(t)$ is the acceleration record, T_1 and T_2 are respectively the beginning and the end of the interval in which the Root Mean Square acceleration (a_{RMS}) at the instant t is obtained. The maximum Root Mean Square acceleration, simply referred to as RMS, is obtained as the maximum $a_{\mathrm{RMS}}(t)$ in the complete length of the acceleration record.

Although comfort criteria based on RMS like Irwin's [24] are widely employed, there is a general lack of information on how to define the boundaries of the interval (T_1 and T_2), specially for traffic-induced vibrations. When considering buildings under wind-induced excitations normally the RMS is

obtained over periods of twenty to sixty minutes. Nevertheless, it seems unreasonable to consider that pedestrians are constantly engaged in either walking or standing on the bridge [24]. An averaging time of one second (i.e. $\Delta t = T_2 - T_1 = 1$s) has been proposed for building walkways without vehicular traffic [31].

Most of the applications to VBI models are focused on the impact factors due to the traffic action in different types of structures [13, 14]. Few research works on comfort analysis pay attention to the influence of the bridge characteristics on the SLS of vibrations, providing clear recommendations on how to limit excessive accelerations. Moghimi and Ronagh [29] observed the strong increment of vibrations in a multi-girder composite deck when the stiffness of the neoprene supports is unreasonably low. These authors suggested a minimum girder depth $d = L/20$ to limit the vibrations based on the Irwin's comfort criterion for storm conditions. Khan [2] also suggested that shallow beams with small d/L ratios are likely to result in higher deflections and cause excessive vibrations. More recently, Nassif *et al.* [9] observed that increasing the slab thickness is more efficient in reducing the peak accelerations than increasing the deck depth. The majority of these studies are focused on the response of the bridge under the action of a single vehicle. Very few studies consider also the vibration in the vehicle cabin and even less account for the effects of the vehicle wheels crossing the bridge joints. Cai *et al.* [32] observed the importance of transition slab settlements on the traffic-induced bridge deflections by means of simple permanent shifts in the roughness profile, without detailing the articulation of the bridge joints. Unfortunately, the acceleration in the vehicle was not reported.

This work is focused on three different aspects:

1. *The methodology for the analysis of bridges under traffic loads.* The paper presents a general framework of VBI analysis to realistically include the hammering effects of the vehicles. The flexibility of the transition slab, the rotation and levelling errors at the bridge joints and the effect of the supports are included in the model, as well as the pavement roughness profiles filtered by the vehicle wheels at these locations. The influence of the exposure time on the comfort assessment is discussed, and a new design parameter to account for the acceleration in the entire footpath surface is proposed.

2. *The vibrations perceived by pedestrians and vehicle users in composite bridges.* A benchmark case-study that represents this bridge typology

5

for short and medium spans is proposed. The key importance of high-order vibrational modes is observed in the accelerations of the deck, discouraging the traditional deflection-based approaches. The number of vehicles to be included in the analysis, the critical road lanes and the effect of the pavement maintenance are explored from the point of the bridge users' comfort.

3. *The definition of design criteria for this bridge type to fulfill the SLS of vibrations.* In order to define a whole structural-type and obtain applicable design recommendations (in Section 7.4), multiple geometrical and mechanical parameters have been modified from the benchmark problem. Among them, the support conditions, the slab thickness, the girder depth, the slab cantilever slenderness, the span length and the spacing and the depth of the transverse beams.

2. Framework of vehicle-bridge interaction analysis

A general methodology to perform VBI analyses is proposed here, accounting for the realistic response of the vehicles before, during and after crossing the bridge. To this end, the numerical model is not only limited to the bridge and the vehicle but it is extended to the approaching platforms, transition slabs and bridge joints. The proposed analysis framework shown in Figure 1 relies upon the accurate definition of the bridge and vehicle's mass, damping, stiffness, and their interaction in a Finite Element environment. It is therefore directly applicable to any type of bridge and vehicle. The three stages of the methodology are described in the following paragraphs.

Stage 1 (pre-processing): Independent pavement roughness profiles are generated with different cut-off frequencies at the bridge and the approaching platforms to represent the different paving stages. After this, the profiles are connected at the bridge joints (assumed flat), where possible construction levelling errors can be introduced by vertical shifts of the bridge profile (δ_c in Figure 1(b)). Finally, the filtering effect of the wheel-size is introduced by applying the disk-model [21] to the total pavement profile, describing the transition of the wheels between the approaching platforms, the bridge joints, and the deck (Figure 1(b)). Further details about the generation and filtering of the roughness profiles are included in Section 6.

Stage 2 (analysis): Firstly, the self-weight of the vehicle and the permanent load of the bridge is statically applied, ensuring the contact between the vehicle wheels and the platform surface. Secondly, a constant velocity (v)

is applied to the vehicles in the dynamic analysis, with each wheel following the defined roughness profile. The vehicle is modeled as a multibody system with 7 DOF [8, 11]. The model is able to capture the vehicle pitch, roll and heave rigid body motions, as well as the flexibility and damping of its tyres and suspensions. The vehicle interacts with the transition slab and the bridge due to their flexibility, and the forces transmitted by the tyres depend on the bridge (or the platform) deflection and the dynamic response of the vehicle. The result is a nonlinear coupled system of differential equations that can be expressed in matrix form as:

$$\begin{bmatrix} \mathbf{M}_v & \mathbf{0} \\ \mathbf{0} & \mathbf{M}_b \end{bmatrix} \begin{Bmatrix} \ddot{\mathbf{x}}_v \\ \ddot{\mathbf{x}}_b \end{Bmatrix} + \begin{bmatrix} \mathbf{C}_v & \mathbf{0} \\ \mathbf{0} & \mathbf{C}_b \end{bmatrix} \begin{Bmatrix} \dot{\mathbf{x}}_v \\ \dot{\mathbf{x}}_b \end{Bmatrix} + \begin{bmatrix} \mathbf{K}_v & \mathbf{0} \\ \mathbf{0} & \mathbf{K}_b \end{bmatrix} \begin{Bmatrix} \mathbf{x}_v \\ \mathbf{x}_b \end{Bmatrix} = \begin{Bmatrix} \mathbf{f}_v^G \\ \mathbf{0} \end{Bmatrix} + \begin{Bmatrix} \mathbf{f}_v^C \\ \mathbf{f}_b^C \end{Bmatrix} \quad (2)$$

where $\mathbf{M}$, $\mathbf{C}$ and $\mathbf{K}$ are respectively the mass, damping and stiffness matrices. Subscripts 'b' and 'v' refer to the bridge (or the platforms) and the vehicle, respectively. $\mathbf{f}_v^G$ is the external force vector in the vehicle due to its self-weight, $\mathbf{f}_v^C$ is the force vector in the vehicle resulting from the interaction with the bridge, and $\mathbf{f}_b^C$ represents its counterpart in the structure, obtained by the action and reaction principle. Since the position of the vehicles is time-dependent, the interaction is solved numerically in time-domain as described in Figure 1. At every instant t_i, the position of each wheel (represented by nodes) and the contacting surfaces of the deck (or the platform) are identified. Next, the kinematic relations are set up to enforce the contact and obtain the interaction forces ($\mathbf{f}_v^C$ and $\mathbf{f}_b^C$) using the augmented Lagrange method. The model accounts for a possible loss of contact between the deck and the tyres (not observed in the analyses) but not for lateral sliding effects in the wheels. The coupled equations of motion in Eq. (2) are directly integrated at every step time by means of the implicit HHT algorithm [33] implemented in Abaqus [34]. The step time employed in the analysis after the first vehicle accesses the bridge is fixed as 0.001s in agreement with previous research works [14, 32]. This value allows for the accurate description of dynamic responses with frequencies below 50Hz (maximum frequency of interest for the deck vibration [11, 14, 19] and the vehicle vibration [35] in comfort studies) and the precise definition of the roughness profile in the range of velocities considered (60-120km/h). Rayleigh damping is implemented in the structure, with a 0.5% ratio [36] fixed for the 2 and 35Hz frequencies, ensuring that the damping is kept in the range [0.3, 0.8]% for the relevant vibrational modes of the studied bridge (Section 4).

Stage 3 (post-processing): After finishing the analysis, the RMS of the vertical acceleration in the whole deck surface and the vehicle is post-processed for a given value of the averaging time ($\Delta t = T_2 - T_1$) in Eq. (1). The influence of Δt is discussed in Section 5, and some guidance is provided to select this value. The procedure is repeated for each roughness profile and the average and standard deviations of the RMS are obtained. Regarding the response of the bridge, a new design parameter $\text{RMS}_{d,c}$ that represents the acceleration level in the entire surface of the footpath is defined as:

$$\text{RMS}_{d,c} = \frac{\sum_j A_j \text{RMS}_j}{\sum_j A_j} \tag{3}$$

in which A_j is the area adjacent to the jth-node of the deck and RMS_j is the corresponding RMS acceleration at that node, obtained with expression (1).

3. Reference case and initial studies

3.1. Composite ladder-deck reference bridge

A reference 40m-span simply supported composite bridge has been used for this work. The steel - concrete composite deck has two longitudinal edge beams (spaced $s = 10$m) connected transversely by cross beams equally spaced ($s_{tb} = 3$m). The bridge is designed to hold two traffic lanes (3.5m wide) with two lateral sidewalks. Figure 2 includes all the relevant dimensions. The in-situ concrete slab (25cm thick) is cast over permanent formwork (6cm thick). As a consequence of the lack of continuity between precast planks in longitudinal direction, the formwork adds weight but does not collaborate in resisting loading in longitudinal direction. The longitudinal girders have been defined using the preliminary steel-concrete composite bridge design charts provided by [37, 38], which are widely employed by designers. These have been established according to the relevant Eurocodes [36, 39]. The transverse beams have been defined following [38]. The steel employed is S355 J2 and the concrete C40/50 (EN 1992 [40]). The total mass of the deck is 738.2 tones (i.e. 7241.7kN).

The supports in the reference case-study are POT bearings according to the 'classical' layout for simply supported bridges [41] depicted in Figure 3(a). It is important to distinguish between the Sidewalk 1 (over transversely fixed POT bearings) and 2 (over transversely free POT bearings) in Figures 2 and
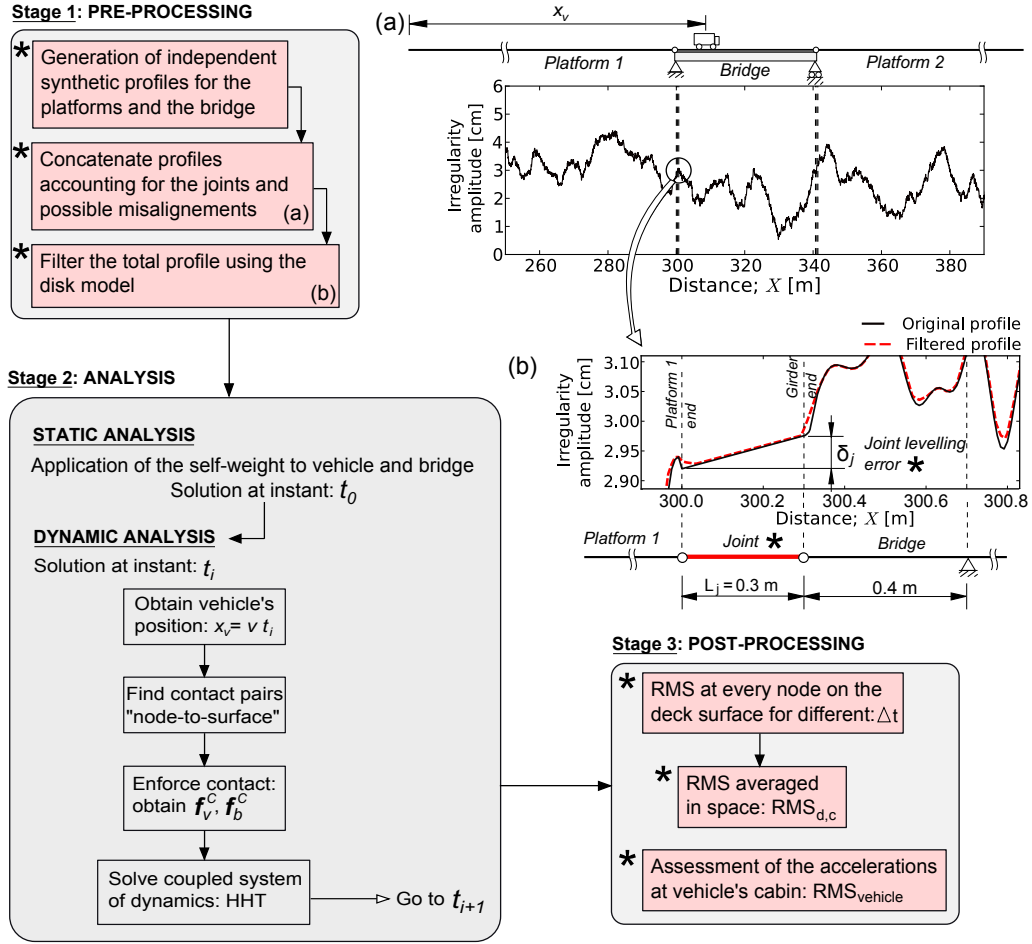
Figure 1: Flowchart including the analysis framework and the innovative concepts (in red and marked with asterisks).
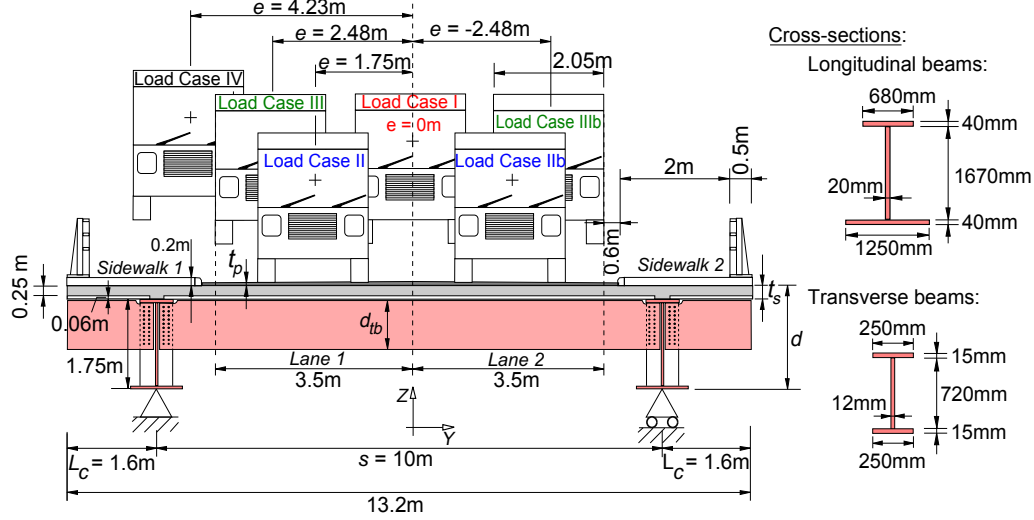
Figure 2: Dimensions of the deck cross-section (abutment level) and Load Cases considered in the study in terms of the vehicle eccentricity, e. The numerical values are included for the reference cross section.

3 as they will present a markedly different vibration. The distance between the center of the supports and the girder end is $L' = 0.4$m (see Figure 4), leading to a total length of the bridge deck $L_t = 40.8$m.

The bridge joints that connect the slab of the deck and the approaching platforms are defined by surface elements that allow for the free movement of both sides and provide continuity on the surface in which the wheel contact is defined. The length of the joint is $L_j = 0.3$m (see Figure 4).

The length of the approaching platform used by the vehicle before accessing the bridge (Platform 1 in Figure 4) is defined for each vehicle velocity in order to ensure that it arrives to the bridge without significant residual movement caused by the application of the self-weight in the first step of the analysis. The length of the exit platform (Platform 2) is defined also in terms of the vehicle velocity so that the complete acceleration histories are at least ten seconds long, starting when the vehicle enters the bridge. This provides the Direct Fourier Transform (DFT) of the accelerations with enough precision in the low frequency range.

Different aspects of this bridge are modified in the following sections in order to perform the parametric analyses, being described when appropriate.
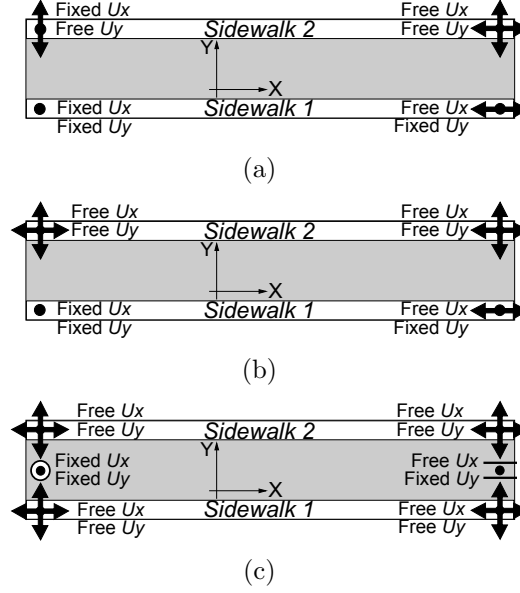
Figure 3: Plan view of the POT support schemes proposed by [41] that have been employed in this study. (a) 'Classical' layout, (b) Statically Determinate layout (referred as SD) and (c) Statically Determinate layout with separate components (referred as 'separate SD').

3.2. The numerical model

The deck steel beams have been defined as three dimensional 'beam' elements rigidly connected to the shell elements representing the concrete slab. The beam elements are defined in the level of the centroids of the longitudinal girders, whereas the shell elements are located in the mid-plane of the in-situ concrete slab, accounting for the offset created by the thickness of the permanent formwork. This model has been tested versus a second model where the beams are defined through shells, obtaining very similar results. Therefore, the former model has been used for the rest of the study avoiding an unnecessary additional computational time. The connection between the concrete and the steel beams is assumed perfect, hence considering that the shear studs transmit completely the shear force in the interface without adding any deformation. This hypothesis is considered reasonable in the linear range, which is to be expected in the SLS analysis conducted in this study.

The vehicle considered in the study is the HA20-44 truck defined by the American Association of State Highway and Transportation Officials

11

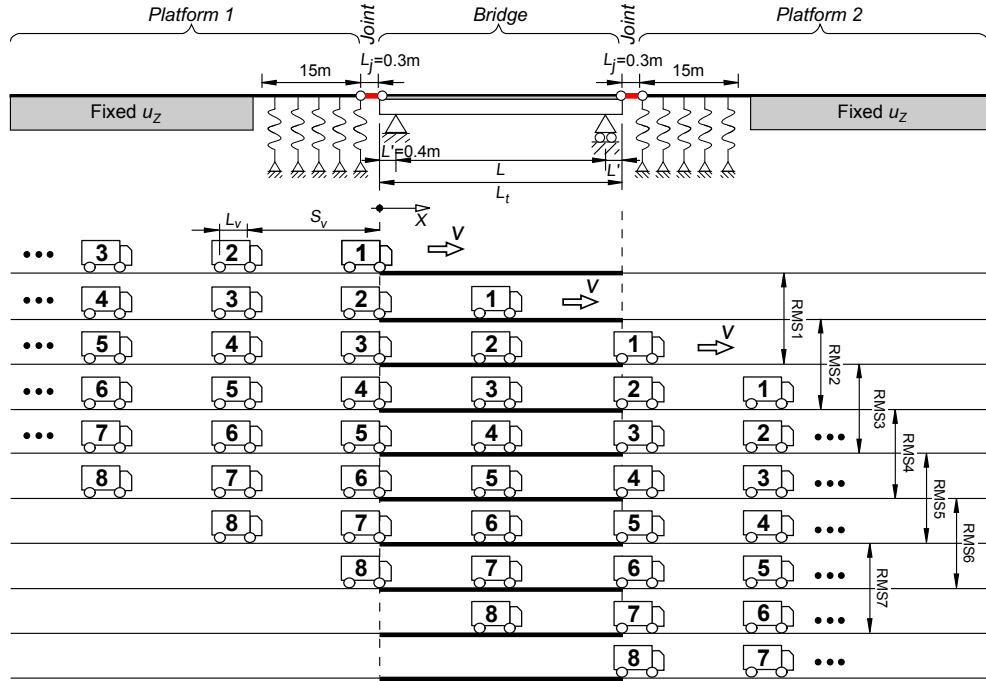Figure 4: Elevation of the bridge and the approaching platforms, including a convoy of eight vehicles equally spaced a distance S_v, running at a velocity v. In the case represented the exit of the ith-vehicle coincides in time with the entrance of the vehicle $i + 2$ ($S_v = (L_t + L_v)/2$), where $L_v = 4.73$m is the distance between the vehicle wheel axes.

(AASHTO) specifications [11]. It is specially relevant for the assessment of the Serviceability Limit State (SLS) of vibrations since it could combine both heavy weight (18.6 tones, i.e. 182.5kN) and high velocities (up to 120 km/h). The frequencies (f) and damping ratios (ξ) of the first vibrational modes of the vehicle MDOF system are as follows: (Mode 1) Body roll, $f_{1,v} = 0.83$Hz, $\xi_{1,v} = 34\%$; (Mode 2) Body pitch, $f_{2,v} = 0.92$Hz, $\xi_{2,v} = 52\%$; (Mode 3) Body pitch and heave, $f_{3,v} = 1.14$Hz, $\xi_{3,v} = 29\%$. Further details of the vehicle model are reported in [8, 11, 14],

3.3. Initial studies

A number of initial studies have been conducted in order to ensure the accuracy of the numerical model and to minimise the traffic-induced vibrations. The following points summarise the main conclusions of these studies:

- A simple two-dimensional beam model representing the longitudinal flexure of the bridge has been developed, describing the vehicle action with moving loads. The maximum acceleration obtained is significantly lower (0.1m/s^2) than in the corresponding VBI analysis. Nonetheless, the results obtained with the simple beam model are questionable as it does not capture the transverse flexure of the slab between longitudinal beams, which is dominant as it will be demonstrated later. The beam model also ignores the pavement roughness, the hammering effect of the vehicle, its mass and its interaction with the bridge. This initial study verified the need of the three-dimensional FEM of the bridge.

- The bridge self-weight deformation increases the traffic-induced accelerations by 8%. Therefore, a precamber (conventionally used in bridge construction) that cancels this initial deformation has been considered in all the analyses.

- At both support sections of the deck the transverse beams are extended (maintaining the same section) to hold the cantilevers of the concrete slab, as represented in Figure 2. This solution is not usually employed in the conventional design proposed by [37, 38] but the vibrations in the sidewalk ends are reduced by 53%, as discussed in Section 7.2. These cantilever steel beams are only included at the diaphragm sections.

- The influence of the transition slab and the abutment's vertical stiffness on the hammering effect of the vehicle, when it accesses or leaves

13

the bridge, has been considered. A detailed FE model (with continuum elements) representing the embankment and the abutment with different soil types was defined. Following this initial investigation, the vertical stiffness of the approaching platforms close to the bridge deck has been defined from this model (in a length of 15m) and employed in the vertical springs of the VBI model (see Figure 4).

4. Influence of the vehicle location across the bridge deck

In this section, vehicles with different eccentricities are considered (see Figure 2), circulating at 90 km/h over a perfect pavement (without roughness). Load cases II, IIb, III, and IIIb represent normal loading scenarios. Load case I has been introduced as a symmetrical reference case, whereas Load case IV has been introduced to consider a hypothetical 3-lane highway bridge without pedestrian walks.

The study of the most contributing modes of vibration is presented first in Figure 5 through the Discrete Fourier Transform (DFT) of the time-histories of acceleration at different points of the deck for Load Case II. It is clear from this figure the reduced contribution of the first vibrational modes in comparison with the large participation of high-order modes (between 18 and 50Hz) that involve the transverse flexure of the concrete slab. This result questions the accuracy of traditional deflection-based methods to assess the SLS of vibrations in conventional composite decks, as the response is not dominated by the first mode of vibration. Acceleration-based methods based on three-dimensional FE analysis seem to be essential to assess the comfort in these conventional bridges. As expected, at locations closer to the abutments the participation of the first vibrational mode (2Hz) is less appreciable. Close to the girder ends, the vibration on the sidewalks is governed by modes with local transverse flexure of the slab (e.g. Mode 3 in Figure 5). This mode of vibration is in turn very sensitive to the possible transverse movement of the supports and it gives large importance to the selection of bearings, as discussed later.

Figure 6 presents the peak acceleration recorded along the edges of the sidewalks and across the deck width. It is remarkable that the dynamic response of the deck is governed by the transverse response of the slab and not by the longitudinal bending. This is suggested by two facts: (1) the almost constant vibration along the deck, with very small accelerations over the steel beams (instead of increasing towards midspan, as it would happen
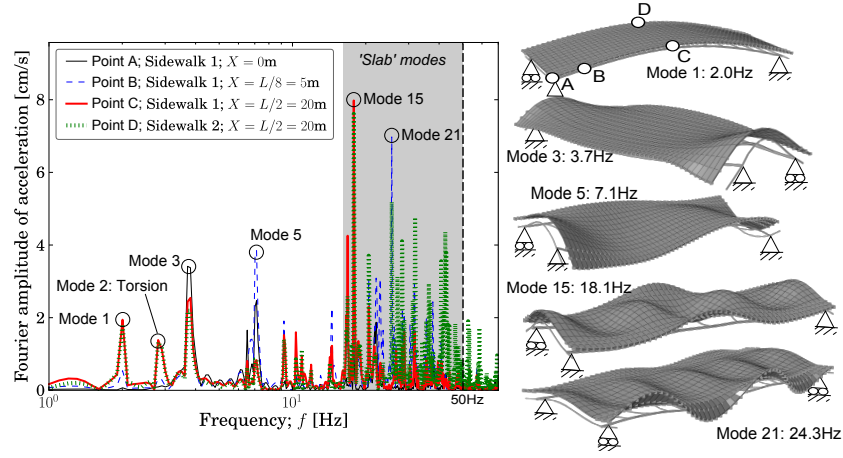
14

Figure 5: Frequency content of vertical acceleration at different points of the deck. The shape of relevant modes of vibration is included, along with the reference points and the support conditions in transverse direction. Load Case II. Perfect road. $v = 90$km/h.

if the response would have been dominated by the first mode of vibration), and (2) the larger accelerations when the vehicle runs with such eccentricities that the load is applied at locations where the relevant modes have larger deformation (i.e. larger in load case I than in load case IV). Previous research works found that vehicles with maximum eccentricity increase the vibrations in bridges in which the global torsional response was found to be important [8, 29]. The interesting result presented in this work adds generality to the previous outcome: the vehicle path that maximises the vibrations in the deck is the one that runs over the areas with maximum deformation in the governing vibrational modes. In the bridges studied in this paper, this position is centered (Load Case I). The section at the first span-octave ($X = L/8 = 5$m) included in Figure 6(b) is typically critical in terms of vertical accelerations due to the participation of the 21-th vibrational mode represented in Figure 5. The acceleration recorded at the deck centreline is much higher than in the footways, however pedestrians are not expected to use that part of the bridge and the vehicle suspension filters the vibration perceived by the vehicle users. It is noticeable that the peak acceleration in the Sidewalk 2 (over transversely free POT supports) is around 2.5 times higher than in the opposite sidewalk.

For a given absolute vehicle eccentricity, the accelerations are 20-30% larger when the vehicle is located closer to the sidewalk supported on trans-
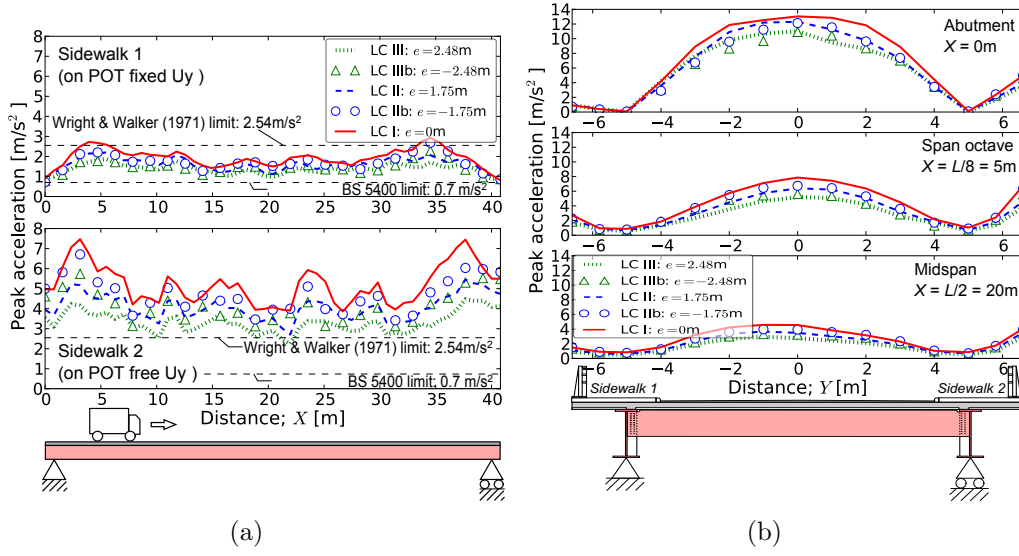
15

Figure 6: Peak acceleration when the vehicle crosses the bridge with different eccentricities. (a) along the sidewalks (edges), (b) across the deck width at different sections. The maximum acceleration limits established by Wright and Walker [3] and BS 5400-2 [28] are included. Perfect road. $v = 90$km/h.

versely free POT bearings (Sidewalk 2) (compare Load Cases II and IIb, or III and IIIb, in Figure 6(a)). In addition, as a consequence of the longitudinal asymmetry of the boundary conditions in the classical configuration of POT supports in Figure 3(a), the peak accelerations in the footways recorded in Load Case II when the vehicle crosses the bridge in opposite direction, i.e. from right to left, are 15% smaller.

The acceleration in the truck has been recorded both in its centre of mass as well as in the cabin (3.153m ahead), where it has been observed that the vehicle pitch could increase the peak vibration by a factor of 2. It has been also distinguished between the acceleration sensed by the driver and the passenger, separated 0.6m from the mid-plane of the vehicle. However, the difference in the vibration at both points is almost negligible (less than 1%) in all the cases studied in this work. Therefore, from hereafter, the vibration of the vehicle will be referred exclusively to the driver. It has been also observed the small influence (up to 4%) of the vehicle eccentricity on the accelerations perceived by the driver (from 2.20 to 2.29m/s^2 in Load Cases I and IV respectively).

Although the critical scenario in terms of deck vibrations is given by the

16

centered vehicle (Load Case I), this is not considered a normal scenario. Load Case II, with the vehicle centered on lane 1, will be therefore considered in the rest of the study.

5. Influence of the RMS averaging time, the comfort criteria, and the convoy length.

The peak acceleration limits established by Wright and Walker [3] ($a_{lim} = 2.54\text{m/s}^2$) and BS 5400-2 [28] ($a_{lim} = 0.5\sqrt{f_1} = 0.7\text{m/s}^2$, where $f_1 = 2\text{Hz}$ is the fundamental frequency of the bridge) are exceeded more than 2.75 and 10 times respectively in Figure 6(a). However, this is not correlated with observation because the case-study represents a very conventional type of bridge in which users' complains are not frequent [10], as reported by [1]. It becomes apparent that comfort criteria based on peak accelerations are questionable as they are caused by single peaks mostly related to the hammering effect of the vehicle entrance and exit. The majority of the research works process the acceleration history using an averaging period, Δt, equal to $T_2 - T_1$ in the calculation of RMS in expression (1). However, very few studies explain the reason to select a particular value of Δt.

It is clear that Δt should depend upon the user characteristics. The question that needs to be addressed is the capacity of the pedestrians, or the vehicle users, to feel short-duration acceleration pulses and the lower duration that the user is able to perceive. The use of the peak acceleration ($\Delta t = 0\text{s}$) is questionable in comfort analysis. In order to shed some light on this important effect, Figure 7 presents the influence of the averaging time (Δt) on the calculation of the RMS employing expression (1). The $a_{\text{RMS}}(t)$ is obtained considering the interval of accelerations recorded before the time t at which it is measured: $T_1 = t - \Delta t$ and $T_2 = t$. The strong reduction of the RMS by increasing Δt is clear from this figure. With the averaging time recommended by [31], equal to one second, the RMS acceleration is around 3.5 times smaller than the corresponding peak value. The discomfort limits observed by Griffin and Whitham [27] for different exposure times are also represented in Figure 7. These results were obtained for accelerations histories with several vibration frequencies (4, 8, 16 and 32Hz) but the influence of the excitation frequency is not significant. Only the result for 16Hz is included in Figure 7, which is close to the vibration frequency with maximum contribution in the structural response (18.1Hz, see Figure 5). The maximum RMS acceleration that can be tolerated increases strongly

by reducing the exposure time. This is an important effect ignored by the most common comfort criteria employed in bridges [24, 28]. These criteria fall extremely on the safe side in this case, leading to over design and to the non consideration of solutions that could be perfectly viable. Considering a conventional velocity of 90km/h, the RMS obtained with $\Delta t = 1$s leads to maximum accelerations in the sidewalks that are within the comfort limits observed by Griffin and Whitham. Research studies on bridge users' comfort in relation to the exposure time are needed. For the rest of this work, the RMS acceleration with an averaging time $\Delta t = 1$s is presented (unless the opposite is stated) as it seems to be supported by previous research [27].
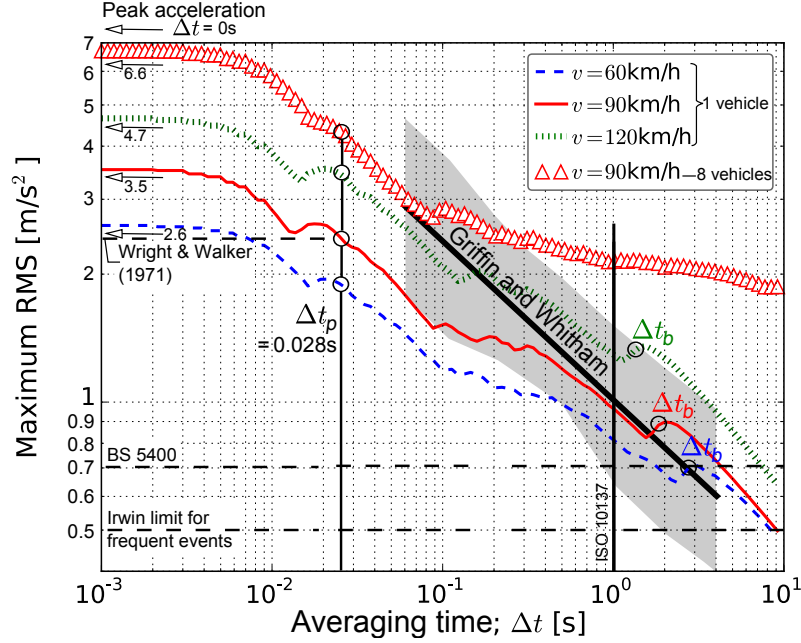
Figure 7: Maximum RMS acceleration in terms of the averaging time (Δt) for three vehicle velocities at Point D (midspan on Sidewalk 2). Perfect road. Load Case II. The colored band represents the tenth and ninetieth percentiles in the comfort experiments conducted by Griffin and Whitham [27], which is centered on the mean value.

Three critical averaging periods in the footways RMS acceleration curves can be identified in Figure 7:

(1) if the averaging interval is smaller than the analysis step-time ($\Delta t < 0.001$s) the maximum RMS acceleration is exactly the peak accelera-

tion, as the averaging interval only captures the acceleration recorded at each time ($a(t)$),

(2) for larger intervals the averaging time covers both the peak and the adjacent smaller values in the acceleration record, strongly reducing the RMS until the averaging time is long enough to include two consecutive peaks. If the dynamic response were dominated by only one mode of vibration, the time between consecutive peaks would be half of its period. In this bridge, several slab vibrational modes are dominant. Nevertheless, considering the most influencing bridge mode (f_{15} = 18.1Hz) leads to $\Delta t_p = 1/(2f_{15}) = 0.028$s, for which a second relative peak in the RMS curves can be identified,

(3) as the interval gets larger, several acceleration peaks and valleys induced by the vehicle are involved in the RMS average and therefore its value decreases at a slower rate. However, this trend changes when the averaging period is able to capture both the entrance and the exit of the vehicle, i.e. $\Delta t_b = (L_{co} + L_t)/v$, where L_{co} is equal to the length of the vehicle (L_v), or the length of the convoy when several vehicles are considered (see Figure 4). When the averaging time is larger than Δt_b it always includes free vibrations in the signal and the structural damping contributes to the rapid decrement of the RMS.

Note that Δt_b depends upon the vehicle velocity whereas Δt_p is an inherent property of the structure. It has been observed that the mentioned values of Δt influence the RMS at different points of the deck, being the decrement of the RMS with the averaging time stronger at the points of the deck close to the abutments, specially for very small values ($\Delta t < \Delta t_p$). This could be explained by the large and localised acceleration pulses introduced by the vehicle at the entrance and the exit of the deck (hammering effect). Regarding the attenuation of the RMS registered inside the vehicle, the same trends described above were observed. However there is no significant decay for $\Delta t < 0.1$s. The influence of Δt_b is stronger in the attenuation of the RMS in the vehicle as the free vibration captured for larger averaging periods are rapidly damped by the vehicle suspension.

When several in-line trucks are crossing the bridge (see Figure 4), the accelerations are increased as represented in Figure 7. The continuous entrance of vehicles makes the attenuation of the RMS with the averaging period less pronounced than in the case with only one vehicle. In order to explore more

19

in detail the influence of the number of vehicles in the accelerations recorded on the sidewalks, Figure 8 presents the RMSi acceleration by fixing the averaging intervals T_1 and T_2 in expression (1) to the instants associated with the entrance and the exit of the ith-vehicle, as it is depicted in Figure 4. In this case the distance between vehicles is defined so that the ith-vehicle is at the span centre when the front axis of the $(i+1)$th-vehicle just arrives to the bridge (see Figure 4). This yields an unreasonably short time between vehicles for the highest velocity (0.68s for 120km/h) but it is considered in order to maximise the dynamic effects. Nevertheless, it has been observed that for the range of reasonable velocities considered (60-120km/h) resonance effects in the bridge are not to be expected due to the high-order dominant frequencies of the response. When a convoy of eight vehicles is considered, the successive entrance of trucks increases the vibration recorded along both sidewalks as expected. However, the increment is more pronounced for the initial vehicles. The increment from seven to eight vehicles is almost negligible (compare RMS 6 and 7). This loading scenario, with convoy of eight heavy vehicles, has a very small probability of occurrence. Nevertheless, it has importance to show how the RMS accelerations are multiplied by almost 2.5 when a convoy of vehicles of these characteristics is considered. The increment in accelerations is considerably higher at span-quarters and midspan, specially on the Sidewalk 1, due to the larger contribution of Mode 15 (see Figure 5) and other slab modes.

Just as the acceleration should be averaged in time, it should be also averaged in space in order to avoid conditioning the design of the bridge due to a localised exceedance of the vibration limits on the sidewalks. Accordingly, the 'design' RMS acceleration in Eq. (3) is defined for this purpose and the results presented in the following. The sum in Eq. (3) is extended along an averaging area, whose study is beyond the scope of this work. For comparison purposes, the area has been extended to the entire sidewalk in this study and simply referred hereinafter as 'design' RMS acceleration: $\text{RMS}_{d,c}$. It has been computed for convoys of trucks crossing the bridge at 60, 90 and 120km/h. Two different spacings between consecutive vehicles (S_v) have been considered: the aforementioned minimum distance $S_v = (L_t + L_v)/2$ and $S_v = 2v + L_v$ (with v in m/s) derived after considering the conventional minimum safety time of 2 seconds between the front axis of a vehicle and the rear axis of the vehicle ahead. Figure 9 synthesises the results by presenting the ratio of the design $\text{RMS}_{d,c}$ acceleration obtained for the convoy and that for only one vehicle. It is clear that the acceleration increases as
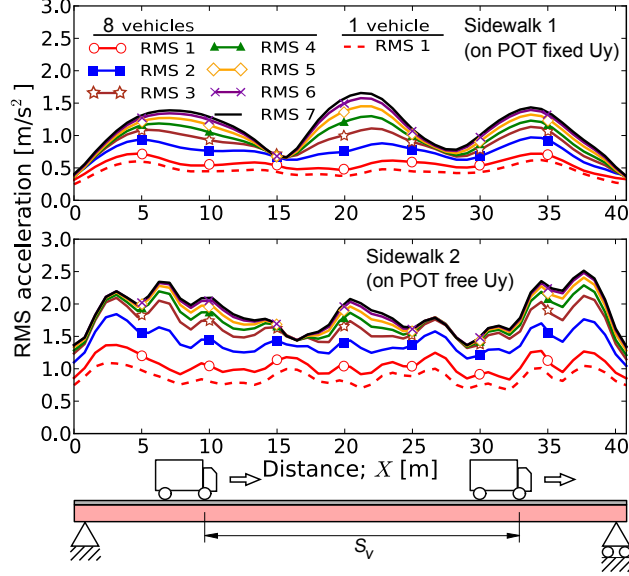
Figure 8: RMSi accelerations (see Figure 4) along the edges of the sidewalks when one or multiple (up to eight) vehicles cross the bridge with the minimum spacing $S_v = (L_t + L_v)/2$. Load Case II. Perfect road. $v = 90$km/h.

successive vehicles cross the bridge. Nevertheless, the vibration increases at a higher rate for the first two or three vehicles (see inflexion points in Figure 9) and it is attenuated for the rest. The acceleration RMS 3, which involves the participation of the first 4 vehicles, represents 81 - 89% of the design RMS$_{d,c}$ acceleration on the sidewalks observed with the convoy of 8 vehicles. Similar values have been observed for peak accelerations at midspan. When the spacing between vehicles is larger the increment of acceleration with successive vehicles decreases. This was to be expected as the free vibrations between the entrance of vehicles are mitigated by the structural damping. In the limit, when the distance between vehicles tends to infinite, the vibration tends to be the one obtained in the case with only one vehicle. It is clear the importance of considering realistic traffic loading (in relation to vehicle types, weights, speeds and spacings), not just one single heavy vehicle, in the assessment of the SLS of vibrations. This leads to further research to be able to define realistic loading scenarios for different road types. For the rest of the paper, only one vehicle crossing the bridge at 90km/h is considered hereafter as the purpose of this work is to study the influence of different features on the vibration of ladder-deck bridges, not to check the SLS of vibrations
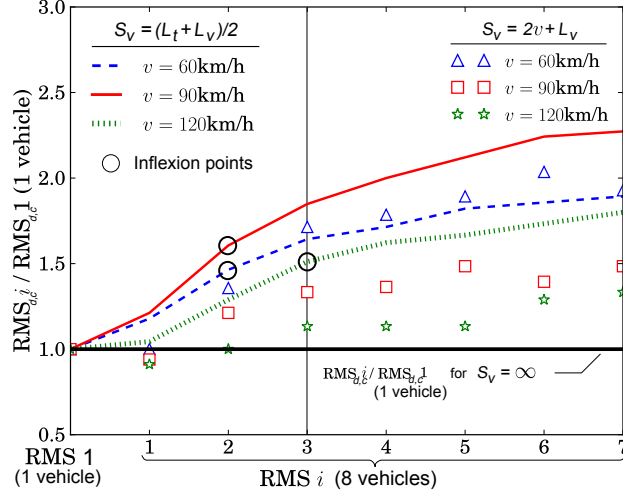
21

of any specific structure.

Figure 9: Ratio between the design RMS acceleration ($\mathrm{RMS}_{d,c}$) averaged for both sidewalks with one and multiple vehicles. The integration intervals involved in the RMS calculation are defined in Figure 4. Load Case II. Perfect road.

6. Influence of the road roughness and the construction levelling errors at the bridge joints

In this section, the pavement roughness is included by means of imposed displacement profiles in the vehicle wheels. The road roughness is generated to match the Power Spectral Density (PSD) function for different road categories (A, B and C). The process is homogeneous and Gaussian with zero mean, based in the inverse Fast Fourier Transform. The profile $r(x)$ is obtained by adding successive sinusoidal functions within the range of frequencies of interest:

$$r(x) = \sum_{k=1}^{N} \sqrt{2G_d(n_k)\Delta n} \cos\left(2\pi n_k x + \theta_k\right) \tag{4}$$

in which x is the position of the point where the profile is defined, n_k is the spatial frequency [cycle/m], N is the number of frequencies included, n_1 and n_N are respectively the lower and upper cut-off frequencies, Δn is the frequency resolution, θ_k is a random phase angle uniformly distributed from 0 to

22

2π, and $G_d(n_k)$ is the PSD function [m³/cycle]: $G_d(n_k) = G_d(n_0)(n_k/n_0)^{-2}$ [8, 12, 13, 32] (where $n_0 = 0.1$ cycle/m is the reference frequency). The value of the PSD function at the reference frequency defines the road category. The following values in m³/cycle are employed in this study: $G_d(n_0) = 16 \times 10^{-6}$ for road A (very good quality), $G_d(n_0) = 64 \times 10^{-6}$ for road B (good quality), and $G_d(n_0) = 256 \times 10^{-6}$ for road C (regular quality). With the objective of introducing potential construction levelling errors between both sides of each bridge joints, the entire roughness profile is generated in three independent sections: one for each of the two access platforms, and one for the bridge deck. The upper cut-off frequency is $n_N = 30$ cycle/m (higher than the traditional value of 10 cycle/m) to account for the possible influence of high-order frequencies and the realistic filtering effect of the wheels with the disk model. The lower cut-off frequency is $n_1 = 0.01$ cycle/m on the platform and $n_1 = 1/2L$ on the bridge deck, in order to take into account the bridge span (L) on the low-frequency roughness. As suggested by Coussy *et al.* [18], the selected cut-off frequencies multiplied by the maximum and minimum speeds chosen for the vehicle (60-120km/h) determine a time frequency interval [0.167-1000]Hz that should contain the frequencies attached to the problem, i.e. the important frequencies of the bridge and the vehicle [1-50]Hz. The distance between consecutive points in the profile is $\Delta r = 8$mm, which allows for enough precision in the definition of the high-order spatial frequencies of the roughness profile. The frequency resolution is $\Delta n = n_1$ [17]. After the generation of the roughness profiles they are connected at both sides of the bridge joints, assumed perfectly flat, and the disk model [8, 21] is used to filter the complete profile.

By modifying the random phase angle θ_k, two different sets of 10 independent profiles are generated for the wheels at both sides of the vehicle (spaced 2.05m transversely). Consequently, we assume the spatial correlation between the roughness of the road to be negligible in transverse direction. In the following results, the mean value of the RMS acceleration obtained by applying each roughness profile is reported. The standard deviation is also included graphically as colored bands centered in the mean value in order to provide information on the dispersion of the results with different profiles.

Figure 10 shows the maximum RMS acceleration along the sidewalks of the bridge for different pavement qualities. The ideal case of a perfectly flat surface is also included for comparison. It is clear that the vibration of the deck is increased by lowering the pavement quality. Table 1 presents the peak and maximum RMS accelerations sensed by the vehicle driver and by the

23

pedestrians along the sidewalks for different cases. This table also summarises the design $\mathrm{RMS}_{d,c}$ acceleration on the sidewalk presented in expression (3). The $\mathrm{RMS}_{d,c}$ on Sidewalk 2 is increased by 4% when the perfectly flat road surface is changed to a real pavement with very good quality (road A). If the surface is deteriorated from road A to road B, the design $\mathrm{RMS}_{d,c}$ acceleration on Sidewalk 2 increases around 10%. Finally, the increment of acceleration from road B to C (regular road) is around 30%. Similar increments of the dynamic response for roads with successively worse quality were reported by Deng and Cai [13] for multi-girder concrete bridges. By exploring the accelerations across the deck width it was verified that the pavement quality affects more the vibration of the deck at locations not used by pedestrians, such as those between longitudinal girders, and specially at these areas close to the abutments. From Table 1, it is also remarkable that the vertical RMS acceleration sensed by the vehicle users is two times higher if the road quality is regular (road C), in comparison to the result obtained in roads with very good quality (road A). Considering the governing frequencies in the vehicle response (vertical modes around 1Hz), Griffin [42] suggests that RMS accelerations above $2\mathrm{m/s}^2$ can be regarded as uncomfortable for the driver and passengers. When the vehicle velocity is 90km/h, if the road quality is regular (type C), this limit would be exceeded.

Construction misalignments in the bridge joint can trigger the hammering effect of the vehicle. This has been studied by means of different offsets in the roughness profiles between the platforms and the bridge, connected by means of a ramp at the joint. For the road A roughness it has been observed that the influence of the joint construction errors in the registered accelerations on the sidewalks is negligible, provided that they are kept under 10mm (maximum misalignment considered). However, the vibrations perceived by the driver and the passengers increase by approximately 15% when the joint error is 10mm, in comparison with the reference case in which the joint is perfectly horizontal. The construction errors at the bridge joint affect more the vehicle response than the structure. This is because the supports are located only 0.4m away from the joint and therefore the impact due to levelling errors is transmitted rapidly to the bearings, whereas the vehicle can only transform this impact into vibration. For the rest of the paper, the joint is assumed to be perfectly horizontal (i.e. with no construction error).
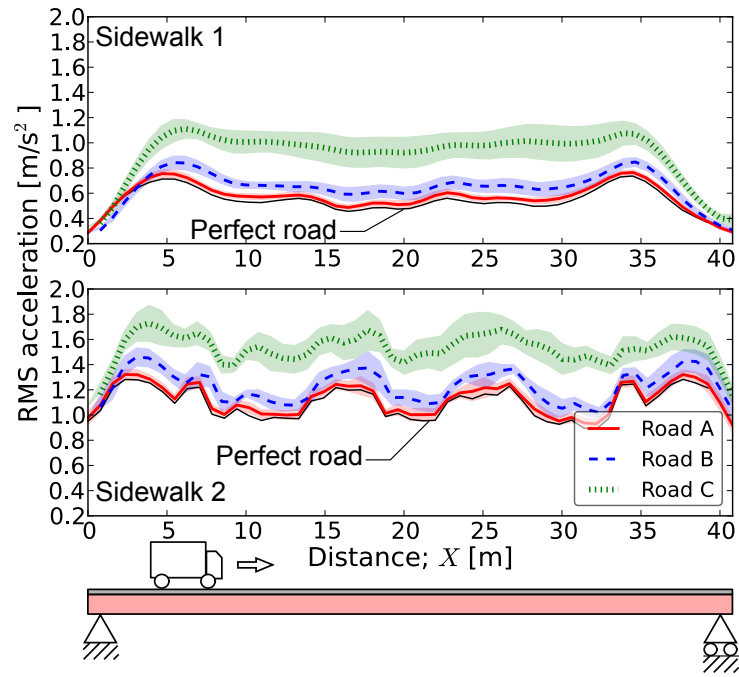
Figure 10: Maximum RMS acceleration along the sidewalks (edges) for different pavement qualities. Load Case II. $v = 90$km/h.

7. Influence of the main bridge parameters

There are several design choices involved in conventional ladder-deck bridges. The objective of this section is to explore their impact on the vibrations sensed by users and to propose design recommendations. All the results presented are those for a typical well-maintained pavement (road A) with no construction levelling error at the bridge joints, considering one truck crossing the structure at 90km/h and centered on Lane 1 (Load Case II).

7.1. Bearing typology

The three POT configurations included in Figure 3 have been studied and compared in Figure 11, along with an additional configuration in which all the supports are completely fixed in longitudinal and transverse directions (referred as 'Fixed' in Figure 11(b)). Furthermore, an additional design solution using Laminated Elastomeric Bearings (LEB) is explored and presented in Figure 11. For this case, circular LEB supports with 450mm diameter and 57mm thickness (41mm thick elastomer and four 4mm thick steel plates) have been designed according to EN 1337-3 [43]. The horizontal and vertical stiffness of LEB supports is represented in the model by elastic springs. The neoprene material properties are $G = 0.9$MPa and $E = 2000$MPa (G and E are the shear and Young's modulus respectively). The increment in stiffness related to fast dynamic actions is usually considered by multiplying these two values by a factor of 2. The influence of the LEB properties on the registered accelerations has been explored by considering three different scenarios: (1) reference value ($G = 0.9$MPa and $E = 2000$MPa), (2) dynamic value ($G' = 2G$, $E' = 2E$), and (3) a stiffer value to account for potential scenarios with very low temperature ($G' = 4G$, $E' = 4E$).

RMS accelerations on Sidewalk 1 are approximately 70% larger when LEB supports are used instead of POT bearings (classical configuration) (see Figure 11(a)). This important increment in the acceleration is observed along the whole sidewalk, leading to a 50% larger RMS$_{d,c}$ on Sidewalk 1 (see Table 1). The effect is caused by the smaller restrain to lateral movements of the LEB supports located close to Sidewalk 1, in comparison to the POT configuration (where the movements were fully restrained). The accelerations on Sidewalk 2 are very similar, as the lateral movements are allowed in both cases. These results are consistent with those conclusions drawn in Section 4. In addition, the strong participation of a vibrational mode with 15.8Hz frequency (see Figure 12(a)), which involves the flexure of the slab and the

longitudinal girders, is responsible for the increment in deck accelerations with LEB supports. With the 'classical' POT configuration, the first slab mode with significant contribution (18.1Hz) does not activate the longitudinal flexure of the steel girders. Moreover, with LEB the response in both sidewalks is similar because the bridge is symmetric in transverse direction (but not the loading). The value of the stiffness of the LEB, within the range considered for this study, does not affect the RMS acceleration in the first quarters of the span. Nevertheless reductions down to 30% are found at midspan (Sidewalk 1) for the most flexible supports considered.

Moghimi and Ronagh [29] concluded that LEB supports that are too flexible in vertical direction increase notably the accelerations in the deck. The present study has found that, while LEB increase the accelerations, it is mainly due to the reduction of the lateral stiffness, when being compared with POT bearings, although vertical and lateral stiffness are related. Figure 11 shows how the largest changes in the RMS accelerations are due to the changes in the transverse stiffness of the bearings (see change in Figure 11(b) from the fixed to the classical POT bearing schemes). This is again related to the fact that the bridge is vibrating as a slab that spans the transverse distance between longitudinal girders. The statically determinate (SD) POT configurations (Figures 3(b) and 3(c)) increase the acceleration by approximately 30% on Sidewalk 1, in comparison with the classical solution (see Figure 11(b) and Table 1) due to a larger participation of the first slab vibrational mode (17 Hz). The statically determinate POT scheme with separate components also lead to an increment in accelerations near the abutments, due to the lower frequency of the first slab mode (13Hz, instead of 18.1Hz as in the classical configuration).

In the solution with sliding POT supports, the friction forces at the PTFE sheet could lock the bearing movements, and make it behave as a 'fixed' POT bearing, if such restraining forces were larger than those reaction forces developed in a fixed POT bearing. Figure 13 shows that, while the longitudinal (X) movement of the supports is clearly allowed, the lateral (Y) forces in the fixed POT bearing can be almost resisted by means of friction forces, i.e. theoretical free movements in the transverse direction would be restrained by friction. Some authors [44] have suggested this blocking effect in POT bearings to justify unexpected values in dynamic load tests. The results of this work confirm this phenomenon, which would in turn lead to a reduction of the vibration on the sidewalks. From hereafter, the results with the classical POT configuration are discussed, adopting the conventional design
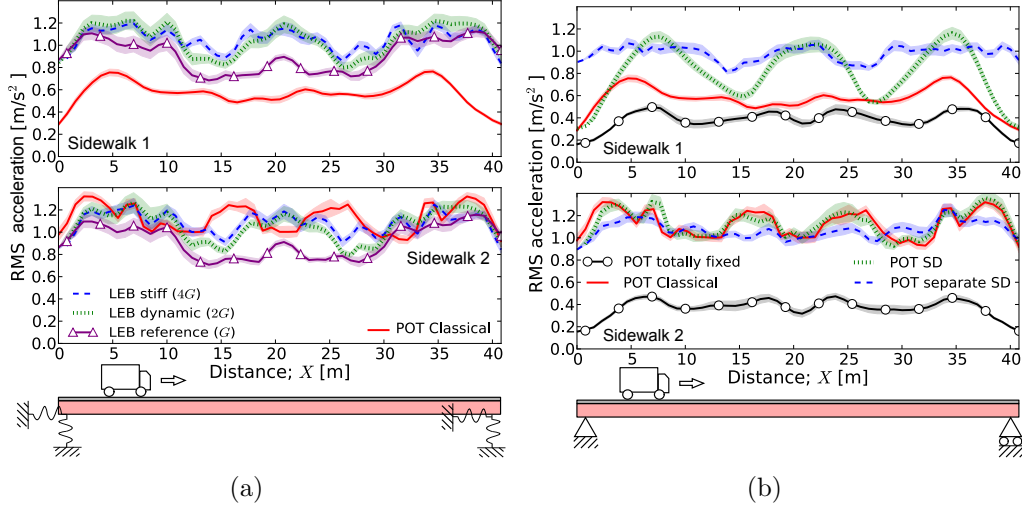
Figure 11: Maximum RMS acceleration along the sidewalks (edges) for different support schemes. (a) LEB supports, (b) POT supports. 'SD' stands for Statically Determinate configuration in the POT scheme (Figure 3). Road A. Load Case II. $v = 90$km/h.

Figure 12: Frequency content of the vertical acceleration of the Sidewalk 1 at midspan for different structural features that affect the response in: (a) transverse direction and (b) longitudinal direction. The reference case is a 40m-span bridge with classical POT support configuration, slab thickness $t_s = 310$mm and cantilever length $L_c = 1.6$m. Load Case II. Road A, road profile No. 1. $v = 90$km/h.

assumption that the sliding bearings release the movement, regardless of the friction forces developed.

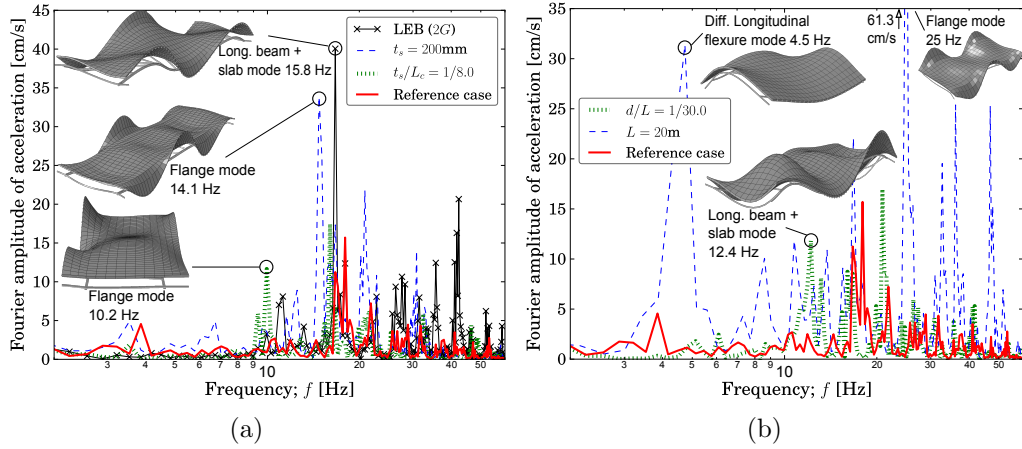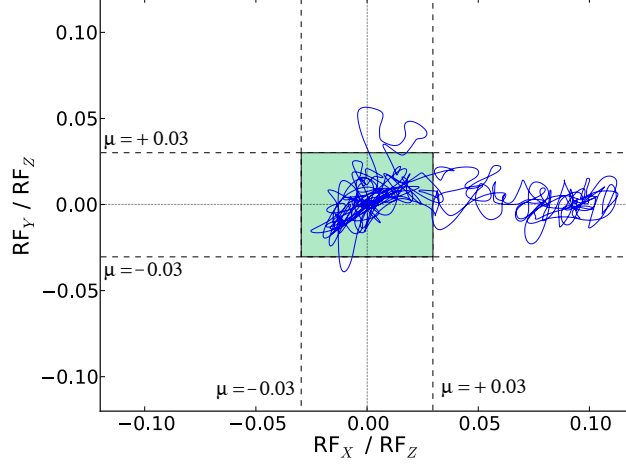Figure 13: Orbit of the ratio between the horizontal reaction in longitudinal (R_X) or transverse direction (R_Y) and the vertical reaction (R_Z) in one of the supports. Model with completely fixed POT bearings. The PTFE coefficient of friction ($\mu = \pm 0.03$) is included [45]. Road A, road profile No.1 . Load Case II. $v = 90$km/h.

Regarding the comfort in the vehicle, fixed POT supports reduce the vibration in the cabin by 20% in comparison with all the transversely free POT configurations considered.

7.2. Structural features with influence on the transverse stiffness: slab and transverse beams morphology

The vibration of the bridge is influenced by the transverse stiffness of the deck, as it is governed by vibrational modes involving the flexure of the slab and the transverse beams. Here, four aspects have been explored due to their close relation to the transverse stiffness of the deck: (1) the slab thickness t_s, (2) the depth of the transverse beams d_{tb}, (3) the spacing between transverse beams s_{tb}, and (4) the transverse spacing between longitudinal girders (s). The results are summarised in Table 1.

The slab thickness strongly affects the mass and the transverse stiffness of the deck. Three different thicknesses have been considered in this study: $t_s = 200$, 310 (reference case) and 400mm (all including the 60mm thick formwork). Note that $t_s = 200$mm is an extreme case included here only for comparison purposes. By increasing the slab thickness the vibrations sensed

by pedestrians on the sidewalks are strongly decreased as it is observed in Table 1. This result is in agreement with [9]. By doubling the slab thickness (from 200 to 400mm) the mass of the deck is increased by 45% and the $\text{RMS}_{d,c}$ is reduced up to 2.3 times on Sidewalk 2 (supported on transversely free POT bearings) and 1.9 times on Sidewalk 1. The study of the maximum RMS accelerations across the deck width shows that the slab thickness affects more the vibrations on the cantilevers (where sidewalks are located) than those at locations between the longitudinal girders. To explain this effect, the DFT analysis on the vibration at midspan (Sidewalk 1) is presented in Figure 12(a). With the thinnest slab (200mm), the vibration is increased specially due to the contribution of a vibrational mode with 14.1Hz that involves mainly the deformation of the slab cantilevers but not the part of the slab between longitudinal girders. Therefore, a slab thickness below 300mm (including formwork) would not be recommended in light of the vibrations recorded on the deck.

The transverse beams are normally designed with workable I sections in which the depth depends upon the depth of the longitudinal girders and the spacing between them. The following transverse beams depths have been explored: d_{tb} =750mm (reference value), 1000mm and 1250mm. The maximum accelerations along the sidewalks for these three cases are reported in Table 1. The design $\text{RMS}_{d,c}$ acceleration on Sidewalk 2 can be slightly reduced with larger transverse beams. However, the influence of the transverse beams is localised near the abutments and the $\text{RMS}_{d,c}$ in Table 1 conceals this local effect. At both ends of Sidewalk 2 the vertical RMS acceleration is reduced by 50% when the transverse beam depth is increased from 750 to 1250mm.

The conventional spacing between transverse beams in ladder-type composite decks ranges from 3 to 4m. In order to have a broad view of the influence of this design parameter, the following values are considered: s_{tb} = 2.5, 3, 3.5 and 4m. The results presented in Table 1 suggest that by reducing the number of transverse beams (i.e. by increasing their spacing) the RMS acceleration recorded on the sidewalks slightly increases. The maximum RMS acceleration along the Sidewalk 2 for a 4m spacing is 27% larger than that for a 3m spacing. However, the design $\text{RMS}_{d,c}$ acceleration is only increased by 11%. Using the slab thickness to reduce the deck vibration is more efficient than modifying the transverse beams, although there is an impact on the deck self-weight that must be considered. In addition, increasing the depth of the transverse beams (d_{tb}) is more efficient than reducing their spacing (s_{tb}). Reducing the spacing will increase the number of beams and it

will also increase the construction costs due to the increment in the number of connections.

The relative length of the cantilevers L_c (and consequently the spacing between longitudinal beams, s) has been modified in order to consider different configurations of the transverse section (maintaining its total width constant). Three different cantilever lengths have been explored: $L_c = 1.6$m (reference case), 2.0m and 2.5m, which configure cantilever slenderness of $t_s/L_c = 1/5.2$, $1/6.4$ and $1/8$ respectively. Figure 14 presents the maximum RMS acceleration across the deck width at several sections along the deck for different cantilevers. Larger cantilevers reduce the transverse span between longitudinal girders, resulting in smaller RMS accelerations in this area. However, the vibration tends to increase in the cantilevers. This is due to the stronger contribution of vibrational modes (with 10.2Hz for the dominant mode, see Figure 12(a)) that only involve the flange flexure. The effect of large cantilevers is specially important at the support sections, where increasing the cantilevers from 1.6 to 2.5m reduced the RMS acceleration at the centreline by 25% and increased it on Sidewalk 2 by 45%. In order to limit the vibration on the sidewalks, specially at locations close to the abutments, it is suggested to locate the longitudinal girders as close as possible to the center of the sidewalks. In this case, the conventional spacing of the longitudinal girders in the cross section represented in Figure 2 resulted optimal from the point of view of the SLS of vibrations. If larger cantilevers are provided, they should be connected at the abutment sections to diaphragms that reduce their transverse flexibility.

The transverse cantilever beams supporting the slab flanges at the support sections (which were considered in all the analyses performed so far, as mentioned in Section 3.3) significantly reduce the vertical accelerations on the sidewalks in the first five meters of the deck length. Table 1 presents the peak and maximum RMS accelerations in the case with, and without, the end transverse cantilever beams at the support sections. When the end cantilever beams are displayed, the maximum RMS acceleration is reduced by 14% and 53% on Sidewalks 1 and 2 respectively. Although the $\text{RMS}_{d,c}$ acceleration on the sidewalks is almost unaffected by the end cantilever beams, the strong reduction of vibration at the deck ends (on the sidewalk supported by transversely free POT bearings) justifies the utilisation of these members. In addition, it has been observed that extending the cantilever beams in the entire bridge length does not appreciably improve the vibrations on the sidewalks as the response along the bridge, outside the support area, is dom-
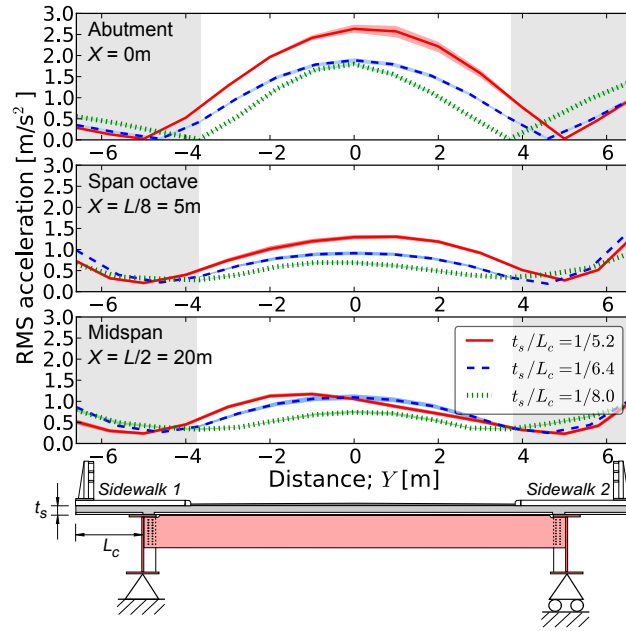
Figure 14: Maximum RMS acceleration across the deck width at different sections for different cantilever lengths. The width corresponding to the sidewalks is highlighted in gray. Road A. Load Case II. $v = 90$km/h.

inated by the slab response between girders, and not by flange vibrational modes. Therefore, it is recommended to extend the transverse beams to the complete width of the deck only at the support sections.

The structural features analysed in this subsection do not significantly affect the vibrations in the vehicle cabin. This is so because they affect the high-frequency response, controlled by slab modes, which is rapidly filtered by the vehicle suspension.

7.3. Structural features with influence on the longitudinal stiffness: longitudinal beam depth and span length

In this section different structural aspects are modified in order to explore the design limits in which the longitudinal bending of the deck between supports becomes dominant. Maintaining the same span length (40m), the depth of the deck (d) was modified by simply varying the depth of the longitudinal steel girders. In this case the plates are not re-designed to facilitate comparison. The following deck depths (including the 0.31m depth corresponding to the concrete slab and formwork thickness) have been explored: $d = 2.31$m, $d = 2.06$m (reference case), $d = 1.64$m and $d = 1.34$m. The resulting slenderness ratios are $d/L = 1/17.3$, $1/19.4$, $1/24.3$ and $1/30.0$ respectively, which fall in the range of values employed in standard practice (ratios around $1/20$ are more common). Figure 15 shows that the smaller the depth-to-span ratio, i.e. the larger the deck slenderness, the larger the acceleration on the sidewalks. On Sidewalk 1 the design $\text{RMS}_{d,c}$ acceleration is increased by approximately 40% and 80% by increasing the reference deck slenderness to $d/L = 1/24.3$ and $d/L = 1/30$ respectively (see Table 2). The frequency content of the acceleration record at midspan (Sidewalk 1) in Figure 12(b) illustrates how the response of the most slender deck ($d/L = 1/30$) is influenced by a dominant mode of vibration involving longitudinal bending of the beams (in addition to transverse flexure of the slab) and having lower frequency (12.4Hz versus 18.1Hz). In agreement with Nassif *et al.* [9], it is observed that the increment of the girder depth reduces the accelerations due to the stiffness increment. Nevertheless, increasing the girder depth is less efficient than increasing the slab thickness, as it also adds mass. In addition, it has been observed that there is a certain depth of the deck beyond which the vibrations cannot be further reduced by increasing the stiffness of the longitudinal girders. This slenderness has been found to be around $1/20$ in ladder-deck composite bridges, and it coincides with the value proposed by

33

Case	Sub-Case	Sidewalk 1			Sidewalk 2			Driver	
		Peak	RMS	$\mathrm{RMS}_{d,c}$	Peak	RMS	$\mathrm{RMS}_{d,c}$	Peak	RMS
Road	Perfect	2.20	0.74	0.33	5.45	1.28	0.49	2.22	1.10
quality	A	2.23	0.76	0.35	5.51	1.32	0.51	2.41	1.16
	B	2.34	0.85	0.39	5.36	1.46	0.56	3.34	1.31
	C	3.06	1.11	0.54	5.60	1.73	0.72	5.85	2.30
LEB	G	3.57	1.12	0.52	4.18	1.16	0.52	2.39	1.14
properties	$2G$	4.90	1.22	0.56	4.93	1.27	0.56	2.39	1.15
	$4G$	5.37	1.20	0.51	4.66	1.25	0.52	2.40	1.15
POT	Classical	2.23	0.76	0.35	5.51	1.32	0.51	2.41	1.16
configuration	SD	3.57	1.16	0.49	5.73	1.36	0.53	2.40	1.16
	Separate SD	5.73	1.07	0.47	5.20	1.25	0.54	2.44	1.16
	Totally fixed	1.81	0.50	0.24	1.56	0.47	0.24	2.13	0.97
Slab	200 (140)	4.41	1.75	0.69	15.31	2.67	0.94	2.35	1.12
thickness	310 (250)	2.23	0.76	0.35	5.51	1.32	0.51	2.41	1.16
t_s (*) [mm]	400 (340)	2.30	0.76	0.36	4.49	0.97	0.40	2.51	1.21
Transverse	750	2.23	0.76	0.35	5.51	1.32	0.51	2.41	1.16
beam depth	1000	2.35	0.76	0.35	5.81	1.33	0.47	2.42	1.17
d_{tb} [mm]	1250	2.82	0.81	0.36	4.64	1.20	0.46	2.45	1.17
Transverse	2.5	2.69	0.80	0.36	6.96	1.68	0.53	2.40	1.16
beam spacing	3.0	2.23	0.76	0.35	5.51	1.32	0.51	2.41	1.16
s_{tb} [m]	3.5	2.99	0.87	0.36	5.69	1.71	0.56	2.41	1.16
	4.0	2.56	0.81	0.34	6.57	1.68	0.57	2.39	1.15
Cantilever	1.6 [1/5.2]	2.23	0.76	0.35	5.51	1.32	0.51	2.41	1.16
length	2.0 [1/6.4]	3.09	1.10	0.40	5.61	1.54	0.48	2.41	1.16
L_c (**) [m]	2.5 [1/8.0]	2.69	0.84	0.40	7.56	1.39	0.53	2.45	1.17
Cantilever	No cantilevers	2.42	0.87	0.36	6.75	2.02	0.49	2.41	1.16
beams	End cantilevers	2.23	0.76	0.35	5.51	1.32	0.51	2.41	1.16

Table 1: Accelerations for different pavement roughness and features that affect the transverse flexure of the bridge. Units in m/s². The mean values are presented. (*) The slab thickness t_s includes the 6cm thick permanent formwork and the structural thickness of the slab appears in parenthesis. (**) The cantilever slenderness, t_s/L_c, appears in brackets. Load Case II. $v = 90$km/h.

Moghimi and Ronagh [29] for multi-girder bridges. The comfort of the vehicle users can be significantly affected by the deck slenderness (see Table 2). By increasing the deck slenderness from 1/19.4 to 1/30 the RMS acceleration sensed by the vehicle users is 2.5 times larger, and exceeds the admissible limit of 2m/s^2 suggested by Griffin [42]. Figure 12(b) shows that vibrational modes with lower frequencies, closer than those of the vehicle (around 1Hz), have more contribution in the response of the slender deck. This explains why, in this case, the vehicle suspension is less effective in reducing the acceleration that goes from the bridge to the vehicle cabin.
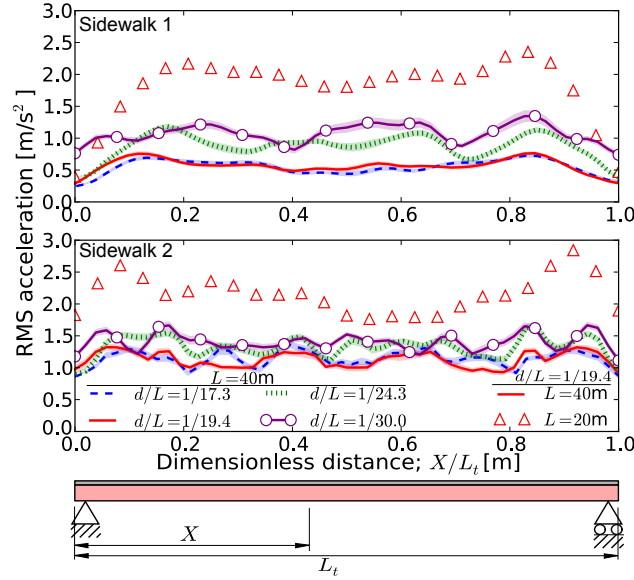

Figure 15: Maximum RMS acceleration along the sidewalks (edges) for different depth to span ratios (d/L) considering the same 40m bridge, and for different spans (L) considering the same $d/L = 1/19.4$. Road A. Load Case II. $v = 90$km/h.

Finally, different span lengths have been considered, re-defining the longitudinal girders according to the same design criteria [37, 38] and slenderness ratio ($d/L = 1/19.4$) used for the reference case. Figure 15 shows that the accelerations at midspan on Sidewalks 1 and 2 for a 20m-span bridge are respectively 4 and 2 times larger than those in a 40m-span bridge. This was to be expected due to the significant reduction in the deck mass (53% smaller). The DFT analysis of the acceleration at midspan in Figure 12(b) shows that in the model with 20m span the response is dominated by two types of vibrational modes that were not observed in the reference bridge with 40m

span: (1) a low-frequency mode of vibration with differential longitudinal flexure of the steel girders (4.5Hz), and (2) multiple high-frequency vibrational modes (above 25 Hz) with deformation mainly in the slab cantilevers. The participation of the longitudinal flexure in the 20m-span bridge can be observed in the shape of the maximum RMS accelerations registered along Sidewalk 1 (Figure 15), increasing from the abutments to the span. The design $RMS_{d,c}$ acceleration on Sidewalk 2 is above $1m/s^2$ (see Table 2), which is the discomfort limit established by [27] for exposure times of 1s (Figure 7). Therefore, it is likely that the vibration induced by the 18.6t truck will result in discomfort of pedestrians in the 20m-span bridge. Moreover, small bridges normally employ LEB and this could further increase the accelerations on the deck as illustrated in Figure 11(a). The lower frequency content of the deck vibration may also explain why the RMS acceleration sensed by the vehicle driver is increased 28% by reducing the span length from 40 to 20m. The accelerations in the bridge with 60m span are smaller on the sidewalks than in the model with 40m, decreasing the $RMS_{d,c}$ acceleration by 26% and 20% on Sidewalks 1 and 2 respectively (see Table 2). The observations of Deng and Cai [13] point to the same direction as they found that the dynamic effect of the vehicle on the bridge decreases as the bridge span length increases up to a certain length. However, it should be noticed that the larger the bridge, the larger the likeness of having additional vehicles, and this could lead to larger accelerations as discussed before.

Case	Sub-Case	Sidewalk 1			Sidewalk 2			Driver	
		Peak	RMS	$RMS_{d,c}$	Peak	RMS	$RMS_{d,c}$	Peak	RMS
Deck	1/17.3	2.42	0.73	0.34	5.54	1.36	0.52	2.05	0.96
slenderness	1/19.4	2.23	0.76	0.35	5.51	1.32	0.51	2.41	1.16
d/L	1/24.3	3.53	1.18	0.49	6.10	1.66	0.61	3.79	1.85
	1/30.0	4.19	1.35	0.62	6.35	1.67	0.69	5.87	2.87
Span length	20	7.71	2.35	0.98	10.84	2.84	1.12	2.92	1.48
L [m]	40	2.23	0.76	0.35	5.51	1.32	0.51	2.41	1.16
	60	1.64	0.62	0.26	4.25	1.21	0.41	2.71	1.24

Table 2: Accelerations for different features that affect the longitudinal flexure of the bridge. Units in m/s^2. The mean values are presented. Load Case II. $v = 90km/h$.

7.4. Design criteria to reduce the traffic-induced vibrations

The proposed design criteria for conventional ladder-deck composite (steel-concrete) bridges are summarised here:

- Support devices have a decisive impact upon the pedestrians' comfort as they affect the shape of the vibrational modes. For this bridge type, support bearings that constrain the lateral movements minimise the accelerations by restraining the vertical displacement on the sidewalks in the most relevant slab vibrational modes. Therefore, transversely fixed POT bearings significantly reduce the accelerations (down to 70%) in comparison to LEB. When the bridge is supported over POT bearings, accelerations are larger on the sidewalk that is closer to the POT bearings with free transverse movement. In addition, it has been observed that sliding POT bearings are likely to be blocked by friction in transverse direction under traffic-induced excitations.

- For this bridge type, the appropriate selection of the slab thickness is one of the most efficient ways to limit the accelerations. A slab thickness below 300mm is not recommended as vibrational modes with deformation of the cantilevers become dominant and reduce the comfort of pedestrians. It was also observed that increasing the depth of the transverse beams is more efficient to reduce the vibrations in the deck than reducing their spacing. It is recommended to locate the longitudinal girders as close as possible to the center of the sidewalks, in light of the study of different slab cantilever lengths. It is also necessary to extend the transverse beams at the support sections of the deck in order to avoid local increments of vibrations on the slab at these points.

- For medium spans (40 m) and decks with very slender girders ($d/L = 1/30$) the RMS acceleration in the vehicle cabin is beyond the admissible comfort limits. The accelerations are reduced in the vehicle and the deck by increasing the beam depth for girder slenderness between $1/20$ and $1/30$ (although this is not as efficient as increasing the slab thickness). For smaller slenderness under this range, larger beam depths do not significantly reduce the accelerations since the traffic-induced bridge response is governed by the transverse flexure of the slab between longitudinal beams.

- When a single vehicle is considered, the traffic-induced acceleration is increased by reducing the bridge span length, specially between 40 and 20m. Nevertheless, the longer the bridge, the higher the probability of having a more demanding loading scenario with several vehicles crossing the bridge at the same time. Additional research is required in order to provide realistic traffic scenarios to be considered in the design of these conventional bridges.

8. Conclusions

This work is focused on the vibrations to which pedestrians and vehicle users are exposed when crossing composite ladder-deck bridges. The reference case-study, plus the multiple geometrical and mechanical parameters considered in the parametric analyses, define a whole structural typology that represents one of the most conventional solutions in infrastructure networks nowadays. These are the main conclusions:

- It has been observed that the vehicle response is significantly influenced by direct actions on the wheels, such as the pavement roughness or construction levelling errors at the bridge joints. Therefore, it is essential for the vibration assessment of highway bridges, where the only users are normally those inside the vehicles, to represent accurately the response of the vehicle and the deck when crossing the bridge joints. To this end, a general analysis framework that is extended beyond the bridge is proposed in this work. The methodology accounts for the flexibility of the transition slab, the articulation of the bridge joints and the filtering effect of the wheels in the roughness profiles.

- The recorded time-history accelerations are filtered because the peak values unreasonably exceed existing limits [3, 28]. It is observed that the RMS accelerations in the deck and the vehicle are very sensitive to the averaging time selected. A new RMS acceleration that is averaged in time and space ($\text{RMS}_{d,c}$) is proposed in order to assess the vibrations in the entire footpaths of the deck.

- The vibration observed in the bridge with 40m-span is dominated by the response of the slab spanning the transverse distance between longitudinal girders and not by their longitudinal flexure. A range of high-order modes of vibration (18-50Hz) involving the transverse flexure of

38

the slab and the transverse beams govern the response. The use of traditional deflection-based approaches to assess the Serviceability Limit State of Vibrations in conventional ladder-deck bridges is questionable, as they are not dominated by the fundamental mode of vibration.

- From the point of view of the assessment of the pedestrian's comfort, the vehicle should be located at the lane where the dominant vibrational modes have larger vertical displacements. In the studied bridges, the maximum traffic-induced acceleration on the sidewalks is achieved when the vehicle crosses the deck centered. This is due to the importance of the transverse deformation in the response. In bridges with larger slab cantilevers, and significant contributions of the longitudinal and torsional modes, the critical position of the vehicle was observed to be eccentric in previous research works [8, 29], which is consistent with this conclusion.

- The accelerations on the sidewalks strongly increase when several in-line vehicles are considered. For a convoy of eight closely spaced heavy vehicles at 90km/h the accelerations are almost 2.5 higher. Nevertheless, the increment is more pronounced for the initial vehicles of the convoy.

- The deterioration of the pavement quality can significantly influence the comfort of pedestrians. Adequate maintenance programmes are recommended to keep the road category between A and B [17].

- The support conditions and the slab thickness control the transverse flexibility of the deck and are critically important for the users' comfort. More detailed design criteria are given in Section 7.4.

9. Acknowledgements

References

[1] C. Roeder, K. Barth, A. Bergman, Effect of live-load deflections on steel bridge performance, Journal of Bridge Engineering 9 (3) (2004) 259–267.

[2] M. Khan, Bridge and highway structure rehabilitation and repair, Mc-Graw Hill, 2006.

[3] R. Wright, W. Walker, Criteria for the deflection of steel bridges, no. 19, 1971.

[4] ASCE, Deflection limitations of bridges, Tech. rep., Proceedings of the American Society of Civil Engineers, rep. No. ST 3 (May 1958).

[5] A. Nowak, H. Grouni, Serviceability considerations for guideways and bridges, Canadian Journal of Civil Engineering 15 (4) (1988) 534 – 537.

[6] A. Shahabadi, Bridge vibration studies. joint highway research project, Tech. rep., Purdue University & Indiana State Highway Commission, rep. No. JHRP 77-17 (September 1977).

[7] J. Smith, Vibration of structures, applications in civil engineering design, Tech. rep. (September 1988).

[8] A. Camara, K. Nguyen, A. Ruiz-Teran, P. Stafford, Serviceability limit state of vibrations in under-deck cable-stayed bridges accounting for vehicle-structure interaction, Engineering Structures 61 (2014) 61 – 72.

[9] H. Nassif, M. Liu, D. Su, M. Gindy, Vibration versus deflection control for bridges with high-performance steel girders, p24-33, in: Transportation Research Board (TRB). Annual meeting, 2011.

[10] L. Oehler, Bridge vibration: Summary of questionnaire to state highway departments, highway research circular, Tech. rep., Highway Research Board. National Research Council, Washington D.C., no. 107 (1970).

[11] S. Marchesiello, A. Fasana, L. Garibaldi, B. Piombo, Dynamics of multi-span continuous straight bridges subject to multi-degrees of freedom moving vehicle excitation, Journal of Sound and Vibration 224 (3) (1999) 541 – 561.

[12] L. Deng, C. Cai, Identification of parameters of vehicles moving on bridges, Engineering Structures 31 (10) (2009) 2474 – 2485.

[13] L. Deng, C. Cai, Development of dynamic impact factor for performance evaluation of existing multi-girder concrete bridges, Engineering Structures 32 (1) (2010) 21 – 31.

[14] X. Zhu, S. Law, Dynamic load on continuous multi-lane bridge deck from moving vehicles, Journal of Sound and Vibration 251 (4) (2002) 697 – 716.

[15] C. Dodds, J. Robson, The description of road surface roughness, Journal of Sound and Vibration 31 (2) (1973) 175–183.

[16] R. Labarre, R. Forbes, S. Andrew, The measurement and analysis of road surface roughness, Tech. rep., Motor Industry Research Association, report No. 1970/5 (1969).

[17] ISO 8608:1995: Mechanical vibration - Road surface profiles - Reporting of measured data (1995).

[18] O. Coussy, M. Said, J. Van Hoove, The influence of random surface irregularities on the dynamic response of bridges under moving loads, Journal of Sound and Vibration 130 (2) (1989) 313–320.

[19] K. Kamash, J. Robson, Application of isotropy in road surface modelling, Journal of Sound and Vibration 57 (1) (1978) 89–100.

[20] K. Captain, A. Boghani, D. Wormley, Analytical tire models for dynamic vehicle simulation, Vehicle System Dynamics 8 (1979) 1–32.

[21] K. Chang, F. Wu, Y. Yang, Disk model for wheels moving over highway bridges with rough surfaces, Journal of Sound and Vibration 330 (2011) 4930–4944.

[22] K. Henchi, M. Fafard, M. Talbot, G. Dhatt, An efficient algorithm for dynamic analysis of bridges under moving vehicles using a coupled modal and physical components approach, Journal of Sound and Vibration 214 (4) (1998) 663 – 683.

[23] C. Heinemeyer, C. Butz, A. Keil, M. Schlaich, A. Goldack, S. Trometer, M. Lukic, B. Chabrolin, A. Lemaire, P. Martin, A. Cunha, E. Caetano, Design of lightweight footbridges for human induced vibrations, Tech. rep., JRC Scientific and Technical Reports, eUR 23984 EN (2009).

[24] A. Irwin, Human response to dynamic motion of structures, The Structural Engineer 56A (9) (1978) 237–244.

[25] C. Roheder, K. Barth, A. Bergman, Improved live load deflection criteria for steel bridges, Tech. rep., National Cooperative Highway Research Program (NCHRP), project 20-7[133] (2002).

[26] S. Zivanovic, A. Pavic, P. Reynolds, Vibration serviceability of footbridges under human-induced excitation: a literature review, Journal of Sound and Vibration 279 (2005) 1–74.

[27] M. Griffin, E. Whitham, Discomfort produced by impulsive whole-body vibration, J. Acoust. Soc. Am. 68 (5) (1980) 1277 – 1284.

[28] BS 5400-2. Steel, concrete and composite bridges - Part-2: Specification for loads (2006).

[29] H. Moghimi, H. Ronagh, Development of a numerical model for bridge-vehicle interaction and human response to traffic-induced vibration, Engineering Structures 30 (12) (2008) 3808 – 3819.

[30] D. Boggs, C. Petersen, Acceleration indexes for human comfort in tall buildings - peak or rms? (1995).

[31] ISO 10137:2007: Bases for Design of Structures - Serviceability of Buildings and Walkways against Vibrations (2007).

[32] C. Cai, X. Shi, M. Araujo, S. Chen, Effect of approach span condition on vehicle-induced dynamic response of slab-on-girder road bridges, Engineering Structures 29 (12) (2007) 3210 – 3226.

[33] H. Hilber, T. Hughes, R. Taylor, Improved numerical dissipation of time integration algorithms in structural dynamics, Earthquake engineering and structural dynamics 5 (1977) 283–292.

[34] Abaqus, Finite element analysis program; version 6.14, Providence USA (2014).

[35] J. McLean, E. Ramsay, Interpretations of road profile-roughness data: review and research needs, Tech. rep., ARRB Transport Research report, ARR 295 (1996).

[36] Eurocode 1 Part 2: Traffic loads on bridges, eN 1991-2:2003 (2003).

[37] R. Mitchell, D. Smith, C. Dolling, Steel-concrete composite bridge design charts for eurocodes, Proceedings of the ICE - Bridge Engineering 164 (4) (2011) 185–194.

[38] British constructional steelwork association ltd., http://www.steelconstruction.org/resources/technical/bridges-preliminary-design.html, accessed: 2014-09-25 (2011).

[39] Eurocode 4: Design of composite steel and concrete structures - Part 2: General rules and rules for bridges, eN 1994-2:2005 (2005).

[40] Eurocode 2: Design of concrete structures. Part 1-1: General rules and rules for buildings, ref. No: EN 1992-1-1:2004 E (2004).

[41] G. Ramberger, Structural Bearings and Expansion Joints for Bridges (IABSE), Vol. 6, ISBN: 3-85748-105-6, Switzerland, 2002.

[42] M. Griffin, Discomfort from feeling vehicle vibration, Vehicle System Dynamics. International Journal of Vehicle Mechanics and Mobility 45 (7-8) (2007) 679–698.

[43] EN 1337-3: Structural Bearings - Elastomeric Bearings, eN 1337-3:2005 (2005).

[44] E. Barzaghi, K. Franklyn, De gasperi and varesine footbridges in milano - dynamic analyses and in situ testing, in: 5th international conference Footbridge2014, 2014.

[45] EN 1337-2: Structural Bearings - Sliding Elements, eN 1337-2:2004 (2004).